# NJC

Accepted Manuscript


This is an *Accepted Manuscript*, which has been through the Royal Society of Chemistry peer review process and has been accepted for publication.

*Accepted Manuscripts* are published online shortly after acceptance, before technical editing, formatting and proof reading. Using this free service, authors can make their results available to the community, in citable form, before we publish the edited article. We will replace this *Accepted Manuscript* with the edited and formatted *Advance Article* as soon as it is available.

You can find more information about *Accepted Manuscripts* in the Information for Authors.

Please note that technical editing may introduce minor changes to the text and/or graphics, which may alter content. The journal's standard Terms & Conditions and the Ethical guidelines still apply. In no event shall the Royal Society of Chemistry be held responsible for any errors or omissions in this *Accepted Manuscript* or any consequences arising from the use of any information it contains.

ROYAL SOCIETY OF CHEMISTRY

www.rsc.org/njc

NJC

PAPER

# Enhancement of Photochemical Heterogeneous Water Oxidation by Manganese Based Soft oxometalate Immobilized on Graphene Oxide Matrix

Received 00th January 20xx,
Accepted 00th January 20xx

DOI: 10.1039/x0xx00000x

www.rsc.org/

Santu Das, Archismita Misra, Soumyajit Roy*

Development of efficient and oxidatively stable molecular catalysts having abundant transition metals at active site is an immediate challenge to synthetic chemists in order to photochemically split water into clean fuels oxygen and hydrogen to serve ever-increasing energy demand. Herein we report a soft-oxometalate (SOM)-based heterogeneous photocatalytic system which effectively performs water oxidation giving oxygen. In the present work we placed a double sandwich type manganese-based molecular polyoxometalate (POM), $Na_{17}[Mn_6P_3W_{24}O_{94}(H_2O)_2].43H_2O$ on an electro active graphene oxide matrix and synthesized a new SOM [$Na_{17}[Mn_6P_3W_{24}O_{94}(H_2O)_2].43H_2O$@ graphene oxide] **1** and performed water oxidation with it. The efficiency of the photocatalytic water oxidation by SOM **1** is almost double than in the case of $Na_{17}[Mn_6P_3W_{24}O_{94}(H_2O)_2].43H_2O$ alone. The rationale lies in the electron accepting nature of the graphene sheets which effectively relay the electrons generated in the water oxidation reaction, thus facilitating the forward reaction and increasing the oxygen yield. Variation of the catalyst-loading, pH and time-dependent experiments are performed on photo catalytic water-splitting. The reaction kinetics is sigmoidal in nature and exhibits the heterogeneous nature of catalysis. The composite catalyst system is observed to be stable towards the reaction conditions.

## Introduction

Water oxidation is one of the most promising routes towards the global goal of alternative energy[1-4]. Many research groups have developed robust catalysts for efficient water oxidation[5-7]. Recently chemists are interested to develop molecular water oxidation catalysts by using cheap and abundant transition metals[6, 8]. Different chemical species are used as catalysts for that purpose e.g. metal organic complexes[9-24], nanomaterials[25-29]; and recently developed polyoxometalates[6, 8, 30-42]. Polyoxometalates (POM) show higher stability in oxidizing environment compared to metal-organic complexes where organic ligands tend to get easily oxidized and thus offer better catalyst stability. Different routes of water splitting have been explored, such as chemical[9, 10], electrochemical methods[2, 43-45] and photoelectrochemical[46-52]. However, photochemical water oxidation seems to be the most facile and clean technique[6, 13, 53, 54].

Recent challenge in photochemical water oxidation by polyoxometalates is to enhance the oxygen generation and increase the Turnover Number (TON) of the reaction[16] . Till now a iridium based complex shows the maximum TON reported by Crabtree and Brudvig [55]. We are interested to observe whether reaction efficiency can be enhanced without changing the active center of catalyst. It is known that POMs can easily be immobilized on the electro active surface to form stable composite system[56]. So, we ask is it possible to employ related composite system to perform water oxidation experiments[29, 33, 57]?

Recently, Hill group developed a similar method using graphene modified electrodes and ruthenium based POM as active catalyst[57]. The graphene modified electrodes shows excellent catalytic activity and high stability toward the electrochemical water oxidation reaction at neutral pH. This work showed enhanced water oxidation reaction electrochemically[57]. Here we ask, is it possible to make a soft oxometalate[56, 58-61] based on polyoxometalate-graphene oxide to enhance the efficiency of photochemical water oxidation?

In our present work we use a manganese based polyoxometalate $Na_{17}[Mn_6P_3W_{24}O_{94}(H_2O)_2].43H_2O$ and synthesize a SOM **1** by immobilizing it on a graphene oxide surface [$Na_{17}[Mn_6P_3W_{24}O_{94}(H_2O)_2].43H_2O$ @ graphene oxide ] **1**. This catalyst shows a turnover number of 22 at pH 8 for WO reaction. This SOM **1** dispersion is prepared by sonication. Formation of composite is confirmed by Raman spectrum, SEM images and EDX. Finally we use this SOM as a photo-catalyst in water oxidation (Fig. 1). Interestingly, we observe that in presence of graphene oxide matrix water oxidation activity of Mn-POM is almost doubled. Detailed account of synthesis, characterization of composite catalyst and of observation related to photochemical water oxidation studies are described in the following sections.

*EFAML, Material Science Centre, Department of Chemical Science, Indian Institute of Science Education and Research Kolkata, Mohanpur – 741246*
*Email: s.roy@iiserkol.ac.in*

This journal is © The Royal Society of Chemistry 20xx



Please do not adjust margins

New Journal of Chemistry Accepted Manuscript

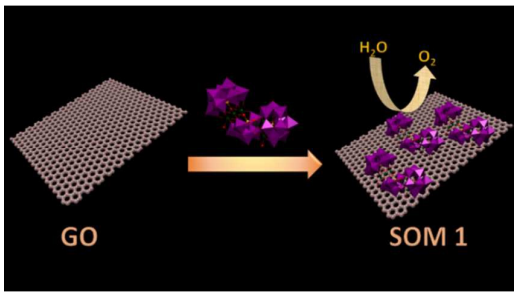


**Fig. 1** Schematic diagram of the overall process.

## Result and Discussion

**Formation of the SOM 1 Composite based on Graphene Oxide**

SOM **1** is prepared by following the classical route of immobilization of POM on an electro active surface[56]. In our present study we initially prepared graphene oxide dispersion in water, to this dispersion $Na_{17}[Mn_6P_3W_{24}O_{94}(H_2O)_2].43H_2O$ (Fig. 2) was added and the mixture was sonicated to finally get the composite SOM **1**, which forms a stable dispersion. Composite formation was characterized by using Raman spectroscopy, SEM images and EDX spectrum.

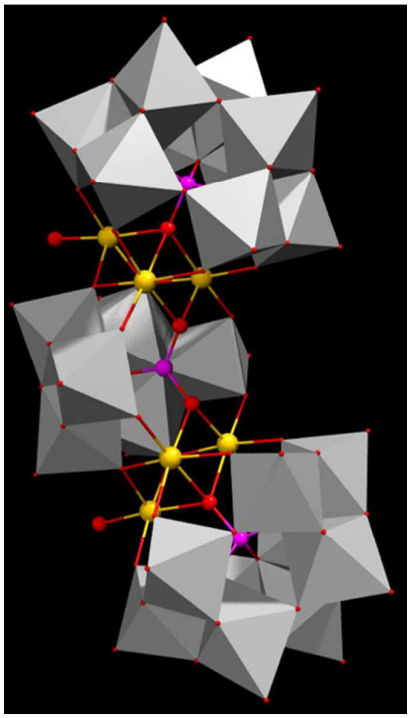

**Fig. 2** Single crystal structure of POM constituent of SOM **1.**

**Scanning Electron Microscopy (SEM): Morphology of SOM 1**

GO shows nano sheet type morphology. It is observed from scanning electron microscopy (Fig. 3a). The SOM **1** shows nanospheres embedded on graphene oxide layers (Fig. 3b). The white bright spot indicate the clustering of POM, suggesting that POM units are may attached to the surface of GO by electrostatic interaction, as GO has electron deficient surface (positively charged) and POM are large polyanion (negatively charged). This further indicates the formation of composite in the reaction system.

From the EDX data we can also infer that the molecular integrity of POM is intact in SOM **1**. [Note: manganese, phosphorus and tungsten are present in expected correct ratio of POM in SOM **1**(Fig. 3c).]

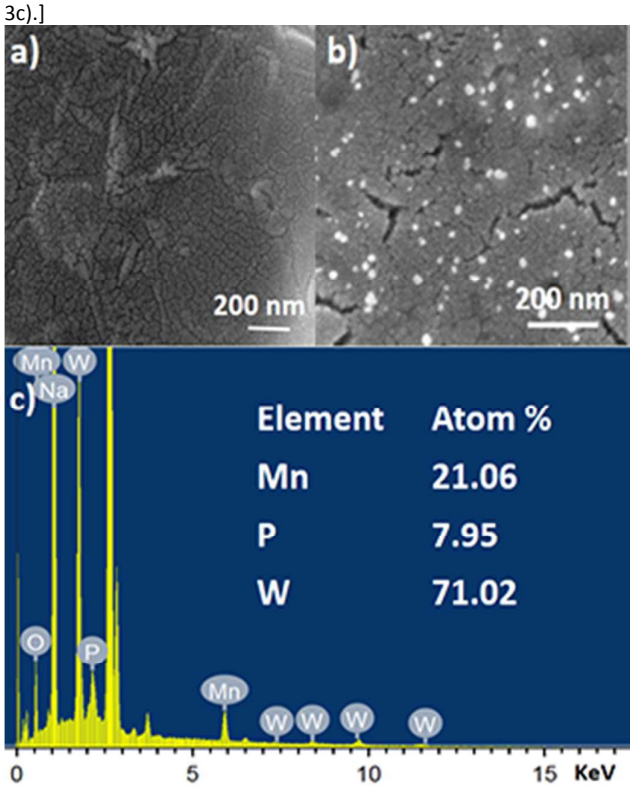


**Fig. 3** SEM images of a) Graphene oxide surface. b) SOM **1**, defined by aggregate nanospherical POMs immobilized on the graphene oxide layers. c) EDX spectrum of SOM **1**.

**HATR-IR Spectroscopy and Stability of POM in SOM 1**

HATR-IR spectroscopy of SOM **1** and also HATR-IR spectroscopy of the POM constituent were performed. It was observed that few broad bands were obtained in each case in the IR spectrum. This broadness is possibly due to the low concentration of the sample in dispersion. Here we observed common peaks for POM and SOM **1** at 1637, 693, 569, 496 $cm^{-1}$ respectively (Fig. 4a). Thus from the IR-spectrum we can conclude that the POM constituent remain intact in the SOM **1** and stable after composite formation and no catalyst is degraded at all. We further performed the UV-VIS spectroscopy to check in change in energy gap in POM constituent after the composite formation.

**UV-VIS Spectroscopy of POM Constituent and SOM 1.**

We performed the UV-VIS spectroscopy of SOM **1** and POM constituent in water. For both POM and SOM **1** we got absorbance the maxima at 250 nm (Fig. 4b). Thus it may be concluded that the band gap of the POM constituent does not change in composite SOM **1**. Which further proves the stability of POM constituent in SOM **1** because if it was dissociated to other cluster unit then there should have been clear difference in the UV-VIS spectrum obtained.

**Raman Spectroscopy and the Nature of SOM 1**

We now want to show the effective formation of SOM. Raman Spectra (Fig. 4c) of the $Na_{17}[Mn_6P_3W_{24}O_{94}(H_2O)_2].43H_2O$, graphene oxide and the SOM **1** composite were taken, for SOM **1** we

New Journal of Chemistry Accepted Manuscript



This journal is © The Royal Society of Chemistry 20xx

Please do not adjust margins

observed 4 peaks at 516, 949, 1379, 1628 $cm^{-1}$ respectively. We assign those peak as following: 516($\nu_{as,\ Mn-O}$), 949($\nu_{W=O}$) and the other two peaks at 1379 and 1628 $cm^{-1}$ for disorder and graphitic nature of graphene oxide respectively. These peaks are blue shifted compared to that of the spectrum of graphene oxide and $Na_{17}[Mn_6P_3W_{24}O_{94}(H_2O)_2].43H_2O$ alone.

Raman spectrum of $Na_{17}[Mn_6P_3W_{24}O_{94}(H_2O)_2].43H_2O$ shows peaks at 495 and 927 $cm^{-1}$ that can be attributed to following modes: ($\nu_{as,\ Mn-O}$), ($\nu_{W=O}$). The characteristic peaks at 1371 and 1618 $cm^{-1}$ are on the other hand due to disorder and graphitic nature of graphene oxide respectively. This shift in spectrum might indicate that there may be possible presence of interaction between POM and graphene oxide layer in SOM **1**. In our system electrons are probably transferred from $Na_{17}[Mn_6P_3W_{24}O_{94}(H_2O)_2].43H_2O$ to graphene oxide[62, 63]. This was further explained by CV. We conclude from this shift that in SOM **1,** graphene oxide may act as electron acceptor and $Na_{17}[Mn_6P_3W_{24}O_{94}(H_2O)_2].43H_2O$ may act as electron donor. Raman spectrum also reveals that SOM **1** is not a physical mixture of both constituents' graphene oxide and POM but an assembly of the two in molecular level.

**Cyclic Voltammogram of the Catalyst**

To further monitor the stability of POM constituent in SOM **1** we performed CV of SOM **1** and compare it with CV of POM constituent of SOM **1** (Fig. 4d) and it is clearly observed that both are identical, which indicate that redox behavior of POM constituent in SOM **1** remain unaltered and we can also conclude that POM constituent is stable after composite formation. Also we observed that peak current enhanced for SOM **1** which further indicate facile electron transport from POM constituent to GO surface.

**Photochemical Water Splitting**

Photochemical water splitting experiments were performed under UV lamp (λmax= 373 nm) with composite catalyst system. The composites were prepared as mentioned in the previous section. The oxygen evolution was monitored by YSI optical sensor based dissolved oxygen meter and also by cyclic voltammetry. The maximum obtained oxygen is 19.2 µmol for 20% SOM **1** loading at pH=8 in phosphate buffer. The graphene oxide acts as electron acceptor and traps the electrons released in the water oxidation reaction and facilitates electron transport as well.

**Confirmation of Water Oxidation and the Effect of Graphene Oxide**

In our present work SOM **1** absorbed light and go to the excited state, this excited SOM **1** generated hole and electron pair, this hole oxidized water to oxygen in presence of light. After photo illumination Quantitative determination of evolved oxygen was performed by sensing the evolved oxygen (Fig. 5c) using YSI optical sensor based dissolved oxygen meter. For further confirmation of evolution of oxygen cyclic voltammetry (Fig. 5a) was performed by taking the samples after photo irradiation, where a sudden rise of current was observed near +1.2 V with respect to Ag/AgCl reference electrode indicative of oxygen evolution from water. It implies oxidation of water.

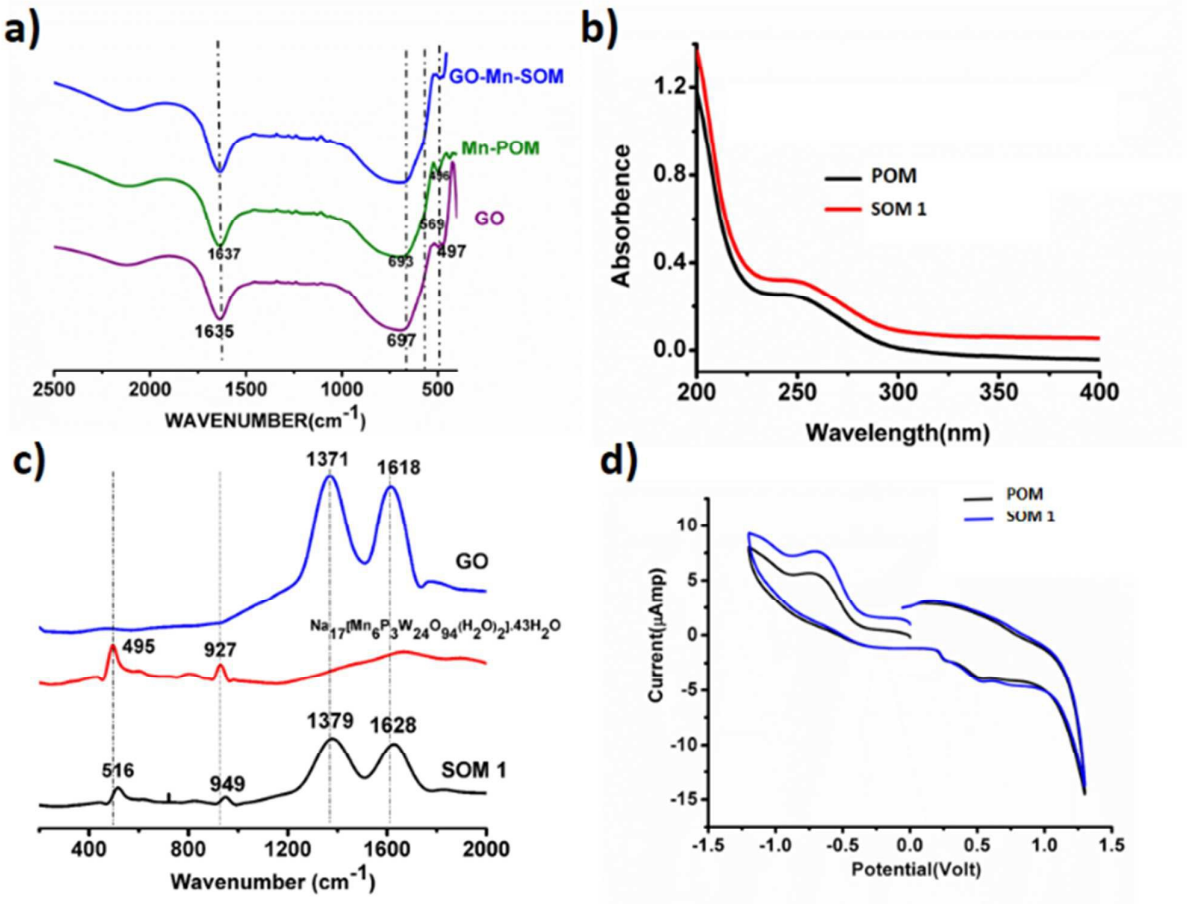


**Fig. 4 a)** HATR-IR spectroscopy of POM constituent, GO, and SOM **1**. b) UV-VIS spectroscopy of POM constituent of SOM **1** and SOM **1**. c) Raman Spectra of the POM unit. $Na_{17}[Mn_6P_3W_{24}O_{94}(H_2O)_2].43H_2O$, graphene oxide and SOM **1**. d) Cyclic Voltammogram of SOM **1** and the POM constituent of SOM **1**.

This jou

New Journal of Chemistry Accepted Manuscript

Please do not adjust margins

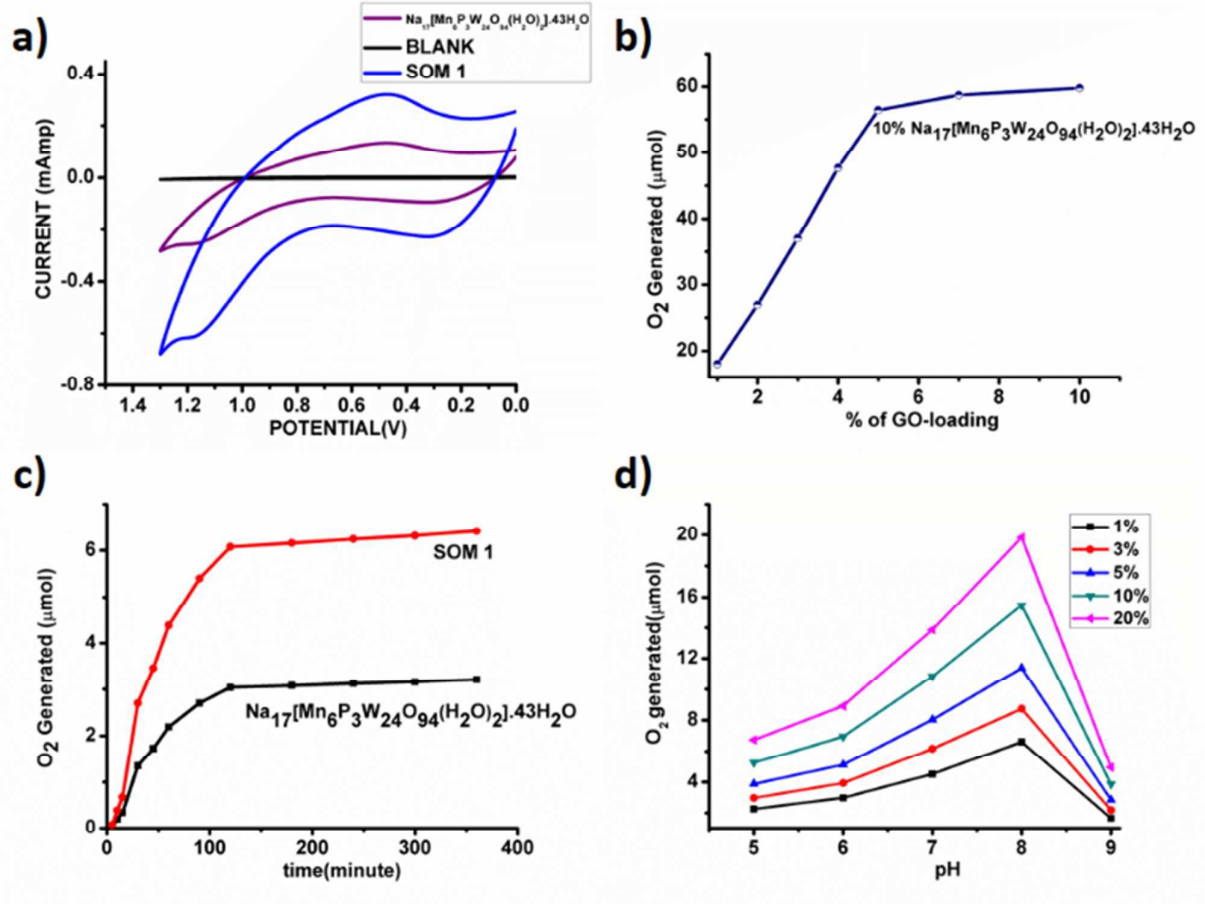


**Fig. 5** a) Cyclic Voltammogram of the water oxidation study by the POM $Na_{17}[Mn_6P_3W_{24}O_{94}(H_2O)_2].43H_2O$ and SOM **1.** b) Extent of oxygen liberated with variation in graphene oxide-loading with constant $Na_{17}[Mn_6P_3W_{24}O_{94}(H_2O)_2].43H_2O$ concentration. c) Comparative oxygen evolution by the POM $Na_{17}[Mn_6P_3W_{24}O_{94}(H_2O)_2].43H_2O$ only and SOM **1.** d) Variation of oxygen yield with pH.

We observe the extent of oxygen evolution is almost doubled in case of the SOM **1** composite catalyst as compared to water oxidation by $Na_{17}[Mn_6P_3W_{24}O_{94}(H_2O)_2].43H_2O$ alone. Using POM alone the maximum amount of oxygen liberated is almost 3.2 µmol for 0.071 µmol loading of the catalyst, with a TON of around 46, whereas in case of SOM **1** composite catalyst system the amount of $O_2$ evolved is almost 6.5 µmol for 0.071 µmol loading of the catalyst with TON of 92 , which is roughly double than that of the POM alone. We thus investigate the role of graphene oxide on water oxidation.

In the next set of experiments, $Na_{17}[Mn_6P_3W_{24}O_{94}(H_2O)_2].43H_2O$ loading was kept constant (10 mg/10 ml in all the catalyst dispersions) and the graphene oxide concentration was increased (Fig. 5b). Here we observe similar type of sigmoidal curve and the maximum $O_2$ generation is almost 58 µmol for 10%SOM **1** loading. The comparative studies clearly show that increase of graphene oxide-loading has a prominent effect on water oxidation. We observed two different aspects (i) upto a certain loading of graphene oxide (5mg) $O_2$ evolution increases to a maximum of 58 µmol. (ii) There after increase of graphene oxide loading there is no further effect on $O_2$ evolution. We explain this as following. With increase in graphene oxide loading the extent of electron relay facilitated by graphene oxide increases, thereby increasing the effective $O_2$ evolution. However beyond a certain threshold of graphene oxide loading the active POM concentration in SOM **1** gets diluted. Hence the evolution of $O_2$ does not increase anymore. Needless to say, that graphene oxide invariably enhances the water oxidation activity. In SOM **1**we also infer graphene oxide most likely provides 1) enhanced active catalytic surface area, 2) facilitates electron transport and there by enhances water oxidation effectively. Also one of the prominent reasons for the enhancement of water oxidation by using GO matrix may due the increase in the effective surface area of the catalyst. In case of SOM **1,** the hydrodynamic radius is around 300 nm (from Dynamic Light Scattering experiment) compared to single SOM having hydrodynamic radius of 130 nm. We have calculated the surface area by assuming the catalyst materials to form nano spheres in dispersion and for a spherical surface we calculated the area by following the equation, surface area = $4\pi R_h^2$. Now we address the problem of how water oxidation is affected with variation in pH and loading of SOM **1** dispersion in the next section.

**pH Dependent Study**

pH dependent water oxidation study reveals some interesting results (Fig.5d).We observe that with increase in pH amount of evolved oxygen increases gradually. At pH 8 we observe the



This journal is © The Royal Society of Chemistry 20xx

Please do not adjust margins

New Journal of Chemistry Accepted Manuscript

maximum yield. On further increase in pH, oxygen evolution decreases abruptly and this may be attributed to the degradation of cluster in higher pH. This observation may be explained by the shift of equilibrium involved with oxygen evolution to the right with increase in pH.

$$H_2O \longrightarrow O_2 + 4H^+ + 4e^-$$

**Catalyst Loading variation Studies**

In this set of experiments, the graphene oxide concentration is kept constant (1 mg/10 ml in all the catalyst dispersions) and the SOM **1** loading is increased to observe the change in the water oxidation. It is observed that with increasing POM loading oxygen evolution increases for a given pH. Nature of the oxygen evolution curve with catalyst loading reveals that initially with increasing catalyst loading oxygen evolution increases rapidly, but after exceeding a certain loading of POM on SOM **1** catalyst (Fig. 6), the rate of enhancement of oxygen evolution in the reaction decreases to some extent. This may be due to the stability factor of the dispersion. More precisely oxygen evolution decreases when phase separation is observed and when we cross the dispersion stability window. This decrease in oxygen evolution is also due to the decrease in active surface area of catalyst.

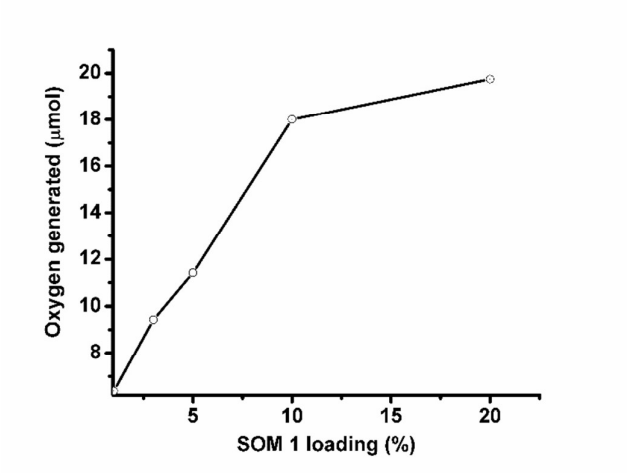


**Fig. 6** Variation of SOM **1** loading at pH-7.

**Time depended studies of oxygen evolution reaction**

Time dependent water oxidation experiments shows general sigmoidal kinetics pattern typical of heterogeneous catalysis reaction, where up to certain limit of time oxygen evolution increases and reaches a plateau (Fig. 7a). There is an induction period of reaction which may be due to light absorption limitation. For excitation of SOM **1** it needs to cross a minimum energy barrier, which is attained after some time therefore initially there is no reaction. When SOM **1** possesses minimum energy for excitation water oxidation starts (Fig. 7b). As water is taken in excess in the reaction, reaction rate only depends on the intensity of light and not on the amount of water present in the reaction medium. At early times of the reaction, i.e., at low light intensity (upto 9.32 mW/ $cm^2$) there is no $O_2$ evolution. However, beyond a threshold light intensity (9.32 mW/ $cm^2$) $O_2$ evolution begins. The induction period (before threshold light intensity) probably simply reflects the time for $O_2$ product equilibration before analysis of evolved $O_2$. It increases in a sigmoidal fashion suggesting co-operative photo-activation of the SOM sites for water oxidation. However with increase in energy density oxygen evolution reaches a saturation. Hence in other words it might be said that water oxidation reaction requires a threshold energy density to begin with, then increases in a sigmoidal fashion implying co-operative photo-activation of the SOM sites finally reaching a saturation with energy density. Thus it implies the water oxidation reaction is topped off after a certain time. Maximum TOF of the reaction is 0.75 $min^{-1}$ which is comparatively lesser than the recently developed photochemical water oxidation using cobalt based POM. This difference in TOF may be due to the involvement of different redox couple in the reaction. Here we observe that the maximum amount of $O_2$ generated is almost 19 µmol for 20% of SOM **1** loading. Now here we ask a question is SOM **1** stable in course of reaction? To determine its stability we measured the Raman spectrum of SOM **1** before and after the completion of reaction. A detailed account of this study is explained in the next section.

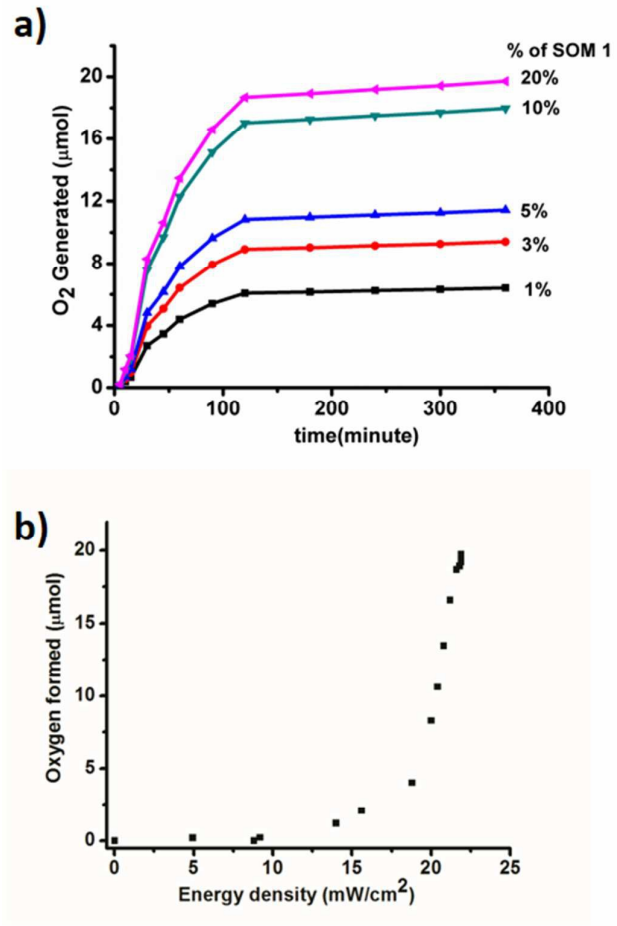


**Fig. 7** a) Concentration and time dependent water oxidation study. b) Plot of energy density of photo reactor with oxygen formed.

**Stability of the Composite SOM Catalyst**

Raman spectroscopic investigations were performed on the SOM **1** composite catalyst before and after the reaction. The spectra are observed to be identical (Fig.8a). We also performed the HATR-IR (Fig. 8b) and UV-VIS (Fig. 8c) spectroscopy of the SOM 1 catalyst after reaction. We also performed cyclic voltammetry (Fig. 8d) with the post reaction dispersion and in all the cases we observed identical spectra compared with the spectra obtained with the

New Journal of Chemistry Accepted Manuscript

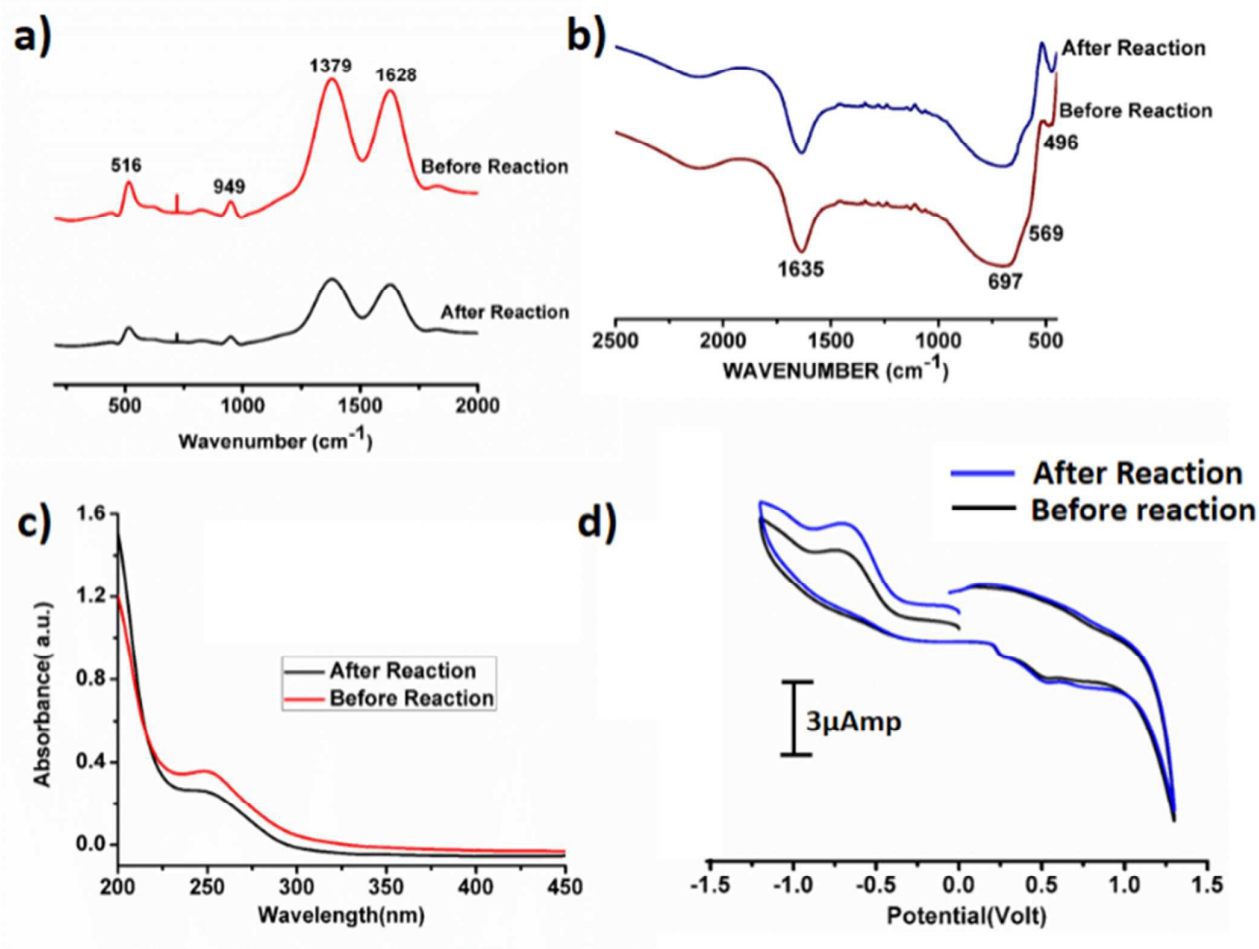


**Fig. 8** a) Raman spectrum of the catalyst SOM **1** before and after the reaction b) HATR-IR spectrum the catalyst SOM **1** before and after the reaction. C) UV-VIS spectrum the catalyst SOM **1** before and after the reaction. d) Cyclic voltammogram of the catalyst before and after reaction.

dispersion SOM **1** before reaction. So we can possibly comprehend that the composite catalyst system remains intact during water splitting reaction. Thus the reported catalyst system is stable under the water oxidation conditions that are used in this study. The POM constituent does not dissociate to form $MnO_2$ or some other fragment. Therefore during photochemical water oxidation reaction it is reasonable to believe that no $MnO_2$ is generated in reaction condition which can possibly oxidize water. Only the POM constituent is clearly responsible for the water oxidation reaction. More experiments and analysis are needed to pin-point the active species, excited species life-time and other deeper mechanistic details which will be performed by us in the future. We also took SEM image (Fig. 9) of the post reaction composite catalyst and observed almost similar kind of morphology with the images taken before the commencement of the reaction.

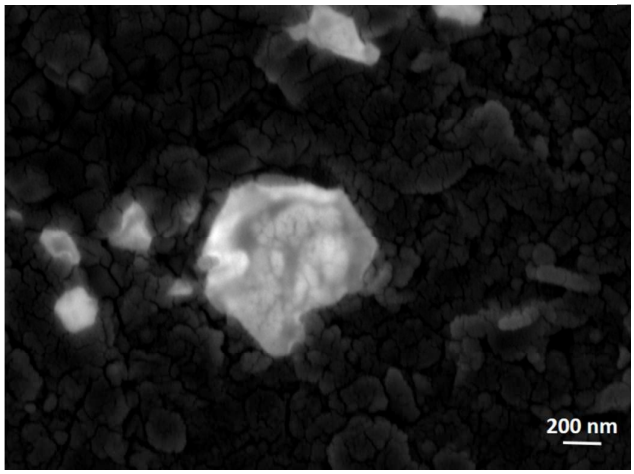


**Fig. 9** SEM image of post reaction SOM **1.**



This journal is © The Royal Society of Chemistry 20xx

Please do not adjust margins

New Journal of Chemistry Accepted Manuscript

**Catalytic Recyclability of SOM 1**

As the catalyst is stable after reaction, we can effectively reuse this catalyst for further catalytic cycles. For this purpose we checked the recyclability upto 10 catalytic cycles and we observed each time equal amount oxygen is evolved in the catalytic cycle (Fig. 10). Therefore the catalyst is completely reusable.

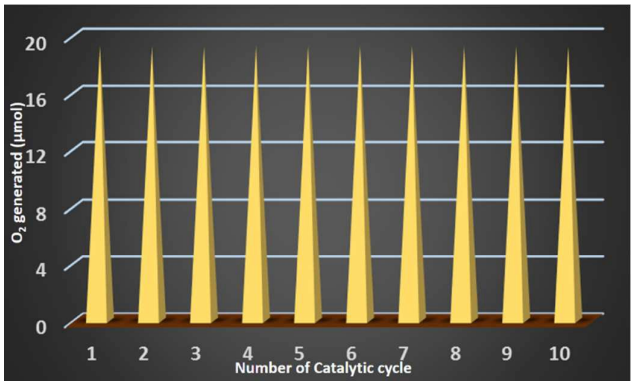


**Fig. 10** Catalytic recyclability of the composite catalyst SOM **1**.

**Mechanism of Evolution of $O_2$ from Water**

Photochemical water oxidations with polyoxometalates generally take place in the presence of an additional photosensitizer and a sacrificial electron acceptor. In our present work, the photocatalytic heterogeneous reaction possibly follows a completely different pathway. Here we need not add any photosensitizer and sacrificial electron acceptor. SOM **1** itself may be absorbing light and going to the excited state which oxidizes water to oxygen (Fig. 11), but elucidation of the actual photophysical mechanism will require additional studies. To further prove that the excited species oxidized water we added catechol in the reaction and observed that the water oxidation ceased under these conditions. This may be due to the fact that catechol oxidation is more favorable compare to water oxidation and therefore water oxidation does not take place in the presence of catechol. The graphene oxide sheets are expected to act as electron acceptor platforms for the electrons generated in the water oxidation process[64, 65] and also enhance the surface area of POM constituent of SOM **1**.

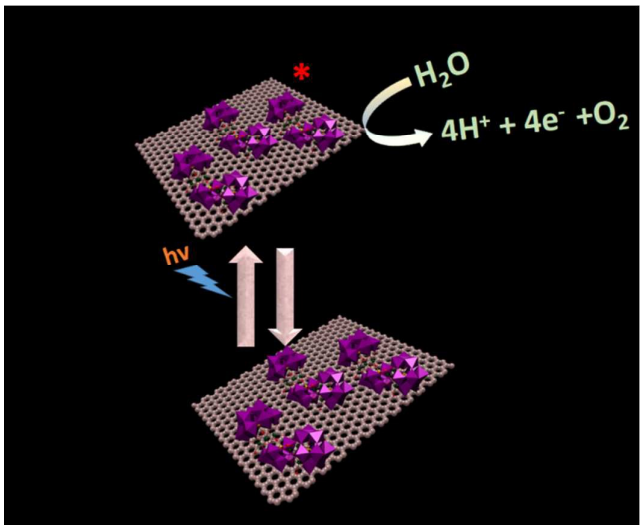


**Fig. 11** Pathway of the photochemical water oxidation.

## Conclusion

To summarize, we have demonstrated the water oxidation by Mn-polyoxometalate (POM) based soft-oxometalate (SOM **1**) dispersion and the efficiency is almost doubled by immobilizing Mn-POM on electro active graphene oxide matrix. The catalyst system acts as water oxidizing agent to generate oxygen under photochemical condition. The graphene oxide layers possibly act as electron acceptor and surface area enhancer and facilitate water oxidation by SOM **1**. Thereafter we describe the effect of catalyst loading and pH on photo catalytic water-splitting. From the kinetics of the reaction we show the operation of heterogeneous mode of catalysis. After demonstrating the stability of the catalyst in course of the water splitting reaction we have proposed the plausible pathway of the catalyst action. Further works are in progress in our laboratory in order to design more SOM based water splitting catalysts.

## Experimental Procedure

**Materials and Reagents**

All the materials were purchased from commercially available sources and used without further purification. All the glass apparatus were first boiled in acid bath then in water and finally rinsed with acetone. All the glass apparatuses were properly dried in hot air oven over-night. Doubly distilled deionized water was used to carry out all the experiments.

**Synthesis of Graphene Oxide**

Graphene oxide was synthesized by improved Hummers' Method[66-68]. Hummers' method[69] ($KMnO_4$, $NaNO_3$, $H_2SO_4$) is the most common method used for preparing graphene oxide. A recent methodology study has modified the process to some extent and improved the efficiency of the oxidation process and this modified Hummers' Method[68] was employed here to synthesize graphene oxide for our experiments.

Concentrated $H_2SO_4$ (69 ml) was added to a mixture of graphite flakes (3.0 g, 1 wt equiv) and $NaNO_3$ (1.5 g, 0.5 wt equiv), and the mixture was cooled using an ice bath to 0 °C. $KMnO_4$ (9.0 g, 3 wt equiv) was added slowly to keep the reaction temperature below 20° C as $KMnO_4$ addition is exothermic. The reaction was warmed to 35 °C and stirred for 7 h. Additional $KMnO_4$ (9.0 g, 3 wt equiv.) was added in one portion, and the reaction was stirred for 12 h at 35 °C. The reaction mixture was cooled to room temperature and poured into ice with 30% $H_2O_2$ (3 mL). The mixture was then purified following the usual protocol of sifting, filtering, centrifugation, decanting with multiple washes followed by a final vacuum drying to give 4.0 g of solid product.

**Synthesis of SOM 1**

1 mg graphene oxide was added in 10 ml water and 2 ml ethylene glycol was added to it for better separation of the graphene oxide sheets. Then it was sonicated for 3 hours at room temperature to prepare graphene oxide dispersion. After that, 10 mg of $Na_{17}[Mn_6P_3W_{24}O_{94}(H_2O)_2].43H_2O$ was added and the dispersion was sonicated for 3 more hours. The stability of dispersion was checked and it was found to be stable.

**Photocatalytic Water Splitting**

Photo catalytic water splitting reactions were performed as follows. In the composite dispersion for water oxidation experiment buffer

New Journal of Chemistry Accepted Manuscript

solution of pH 7 was added. The reaction mixture was then sealed and $N_2$ gas was purged for 3 hours to get rid of the trace amount of oxygen in it. Then the reaction mixture was kept in a photoreactor under UV-light (energy density of the photo reactor is - 19.5 mW/cm$^2$ with λmax = 373 nm) for 2 hours. After irradiation we measured the amount of evolved oxygen in the reaction by YSI optical sensor based dissolved oxygen meter standardized by using degassed double distilled water. Evolution of oxygen in the reaction was further investigated by performing cyclic voltammetry using the irradiated samples. In cyclic voltammetry we observed a sharp rise of current-voltage curve near +1.2 V, which is typically indicative of $O_2$ generation by water splitting.

**pH Dependent Water Splitting**

This experiment was performed by following previous procedure using different buffer solution in the range pH 5 to 9. Measurement of the oxygen evolution was carried out by similar method mentioned earlier**.**

**Characterization Techniques**

**SEM-EDX Microscopy**

SEM measurements were done by drop-casting SOM **1** dispersion on silicon wafer and drying under vacuum for 2 days. Then SEM imaging was performed and images were taken on SUPRA 55 VP-41-32 instrument with the Smart SEM version 5.05 Zeiss software.

**Cyclic Voltammetry**

PAR model 273 potentiostat was used for the CV experiments. A platinum wire auxiliary electrode, a glassy carbon working electrode with surface area of 0.002826 cm$^2$ and an aqueous Ag/Ag$^+$ reference electrode which is filled by saturated KCl solution, were used in a three electrode configuration. Scan rate was 0.5 V/s. The CV spectrum was recorded in the range of 0 to +1.3V. Blank refers to the amount of oxygen present in distilled water in our mentioned reaction conditions. The pH of the medium was 7. 0.1 M KCl solution was used as a supporting electrolyte in all the experiments. All measurements were done at 298 K in inert atmosphere.

**Dynamic Light Scattering Measurement**

Average size of the particle was obtained using dynamic light scattering method in a Malvern Zetasizer instrument. A very dilute solution of SOM **1** was prepared by further dilution of the SOM **1** dispersion and taken in a fluorescence glass cuvette with square aperture and the instrument was set to take 15 runs before measuring the average hydrodynamic radius of the SOM **1**composite**.**

**Raman Spectroscopy**

A LABRAM HR800 Raman spectrometer was employed using the 633 nm line of a He–Ne ion laser (λ = 633 nm) as the excitation source to analyze the sample.

## Acknowledgment

SR gratefully acknowledges the grants from IISER-Kolkata, India, DST-fast track and BRNS-DAE grant.

## References

1. D. G. Nocera, *Accounts of chemical research*, 2012, **45**, 767-776.
2. M. Jacobson, W. Colella and D. Golden, *Science*, 2005, **308**, 1901-1905.
3. L. Hammarström and S. Hammes-Schiffer, *Accounts of chemical research*, 2009, **42**, 1859-1860.
4. L. S. Dennis G. H. Hetterscheid, *European Journal of Inorganic Chemistry*, 2014, **2014**, 568-790.
5. J. J. Concepcion, J. W. Jurss, J. L. Templeton and T. J. Meyer, *Proceedings of the National Academy of Sciences*, 2008, **105**, 17632-17635.
6. Q. Yin, J. M. Tan, C. Besson, Y. V. Geletii, D. G. Musaev, A. E. Kuznetsov, Z. Luo, K. I. Hardcastle and C. L. Hill, *Science*, 2010, **328**, 342-345.
7. Y. Zhao, J. R. Swierk, J. D. Megiatto, B. Sherman, W. J. Youngblood, D. Qin, D. M. Lentz, A. L. Moore, T. A. Moore and D. Gust, *Proceedings of the National Academy of Sciences*, 2012, **109**, 15612-15616.
8. G. Zhu, E. N. Glass, C. Zhao, H. Lv, J. W. Vickers, Y. V. Geletii, D. G. Musaev, J. Song and C. L. Hill, *Dalton Transactions*, 2012, **41**, 13043-13049.
9. L. Duan, F. Bozoglian, S. Mandal, B. Stewart, T. Privalov, A. Llobet and L. Sun, *Nature chemistry*, 2012, **4**, 418-423.
10. L. Francas, X. Sala, E. Escudero-Adán, J. Benet-Buchholz, L. Escriche and A. Llobet, *Inorganic chemistry*, 2011, **50**, 2771-2781.
11. I. López, M. Z. Ertem, S. Maji, J. Benet-Buchholz, A. Keidel, U. Kuhlmann, P. Hildebrandt, C. J. Cramer, V. S. Batista and A. Llobet, *Angewandte Chemie*, 2014, **126**, 209-213.
12. J. K. Hurst, *Coordination chemistry reviews*, 2005, **249**, 313-328.
13. S. Roeser, P. Farràs, F. Bozoglian, M. Martínez-Belmonte, J. Benet-Buchholz and A. Llobet, *ChemSusChem*, 2011, **4**, 197-207.
14. J. F. Hull, D. Balcells, J. D. Blakemore, C. D. Incarvito, O. Eisenstein, G. W. Brudvig and R. H. Crabtree, *Journal of the American Chemical Society*, 2009, **131**, 8730-8731.
15. N. S. McCool, D. M. Robinson, J. E. Sheats and G. C. Dismukes, *Journal of the American Chemical Society*, 2011, **133**, 11446-11449.
16. R. Zong and R. P. Thummel, *Journal of the American Chemical Society*, 2005, **127**, 12802-12803.
17. J. J. Concepcion, J. W. Jurss, M. K. Brennaman, P. G. Hoertz, A. O. T. Patrocinio, N. Y. Murakami Iha, J. L. Templeton and T. J. Meyer, *Accounts of chemical research*, 2009, **42**, 1954-1965.
18. N. D. McDaniel, F. J. Coughlin, L. L. Tinker and S. Bernhard, *Journal of the American Chemical Society*, 2008, **130**, 210-217.
19. J. T. Muckerman, D. E. Polyansky, T. Wada, K. Tanaka and E. Fujita, *Inorganic chemistry*, 2008, **47**, 1787-1802.
20. M. W. Kanan and D. G. Nocera, *Science*, 2008, **321**, 1072-1075.
21. D. M. Robinson, Y. B. Go, M. Greenblatt and G. C. Dismukes, *Journal of the American Chemical Society*, 2010, **132**, 11467-11469.
22. A. Indra, P. W. Menezes, I. Zaharieva, E. Baktash, J. Pfrommer, M. Schwarze, H. Dau and M. Driess, *Angewandte Chemie International Edition*, 2013, **52**, 13206-13210.
23. S. M. Barnett, K. I. Goldberg and J. M. Mayer, *Nature chemistry*, 2012, **4**, 498-502.

New Journal of Chemistry Accepted Manuscript



This journal is © The Royal Society of Chemistry 20xx

Please do not adjust margins

24. A. K. Vannucci, L. Alibabaei, M. D. Losego, J. J. Concepcion, B. Kalanyan, G. N. Parsons and T. J. Meyer, *Proceedings of the National Academy of Sciences*, 2013, **110**, 20918-20922.
25. F. Jiao and H. Frei, *Angewandte Chemie International Edition*, 2009, **48**, 1841-1844.
26. T. Zidki, L. Zhang, V. Shafirovich and S. V. Lymar, *Journal of the American Chemical Society*, 2012, **134**, 14275-14278.
27. R. D. Smith, M. S. Prévot, R. D. Fagan, Z. Zhang, P. A. Sedach, M. K. J. Siu, S. Trudel and C. P. Berlinguette, *Science*, 2013, **340**, 60-63.
28. T. W. Kim and K.-S. Choi, *Science*, 2014, **343**, 990-994.
29. M. Quintana, A. M. López, S. Rapino, F. M. Toma, M. Iurlo, M. Carraro, A. Sartorel, C. Maccato, X. Ke and C. Bittencourt, *ACS nano*, 2012, **7**, 811-817.
30. A. Sartorel, M. Carraro, G. Scorrano, R. D. Zorzi, S. Geremia, N. D. McDaniel, S. Bernhard and M. Bonchio, *Journal of the American Chemical Society*, 2008, **130**, 5006-5007.
31. Y. V. Geletii, Z. Huang, Y. Hou, D. G. Musaev, T. Lian and C. L. Hill, *Journal of the American Chemical Society*, 2009, **131**, 7522-7523.
32. C. Besson, Z. Huang, Y. V. Geletii, S. Lense, K. I. Hardcastle, D. G. Musaev, T. Lian, A. Proust and C. L. Hill, *Chemical Communications*, 2010, **46**, 2784-2786.
33. F. M. Toma, A. Sartorel, M. Iurlo, M. Carraro, P. Parisse, C. Maccato, S. Rapino, B. R. Gonzalez, H. Amenitsch and T. Da Ros, *Nature chemistry*, 2010, **2**, 826-831.
34. M. Murakami, D. Hong, T. Suenobu, S. Yamaguchi, T. Ogura and S. Fukuzumi, *Journal of the American Chemical Society*, 2011, **133**, 11605-11613.
35. G. Zhu, Y. V. Geletii, P. Kögerler, H. Schilder, J. Song, S. Lense, C. Zhao, K. I. Hardcastle, D. G. Musaev and C. L. Hill, *Dalton Transactions*, 2012, **41**, 2084-2090.
36. S. Tanaka, M. Annaka and K. Sakai, *Chemical Communications*, 2012, **48**, 1653-1655.
37. H. Lv, Y. V. Geletii, C. Zhao, J. W. Vickers, G. Zhu, Z. Luo, J. Song, T. Lian, D. G. Musaev and C. L. Hill, *Chemical Society Reviews*, 2012, **41**, 7572-7589.
38. J. Soriano-López, S. Goberna-Ferrón, L. Vigara, J. J. Carbó, J. M. Poblet and J. R. n. Galán-Mascarós, *Inorganic chemistry*, 2013, **52**, 4753-4755.
39. S. Goberna-Ferrón, L. Vigara, J. n. Soriano-López and J. R. n. Galán-Mascarós, *Inorganic chemistry*, 2012, **51**, 11707-11715.
40. J. W. Vickers, H. Lv, J. M. Sumliner, G. Zhu, Z. Luo, D. G. Musaev, Y. V. Geletii and C. L. Hill, *Journal of the American Chemical Society*, 2013, **135**, 14110-14118.
41. R. Al-Oweini, A. Sartorel, B. S. Bassil, M. Natali, S. Berardi, F. Scandola, U. Kortz and M. Bonchio, *Angewandte Chemie International Edition*, 2014, **53**, 11182-11185.
42. J. M. Sumliner, H. Lv, J. Fielden, Y. V. Geletii and C. L. Hill, *European Journal of Inorganic Chemistry*, 2014, **2014**, 635-644.
43. S. Chatterjee, K. Sengupta, S. Dey and A. Dey, *Inorganic chemistry*, 2013, **52**, 14168-14177.
44. Y. Gorlin, B. Lassalle-Kaiser, J. D. Benck, S. Gul, S. M. Webb, V. K. Yachandra, J. Yano and T. F. Jaramillo, *Journal of the American Chemical Society*, 2013, **135**, 8525-8534.
45. S. Dey, B. Mondal and A. Dey, *Physical Chemistry Chemical Physics*, 2014, **16**, 12221-12227.
46. D. K. Zhong and D. R. Gamelin, *Journal of the American Chemical Society*, 2010, **132**, 4202-4207.
47. S. Hoang, S. Guo, N. T. Hahn, A. J. Bard and C. B. Mullins, *Nano letters*, 2011, **12**, 26-32.
48. W. J. Jo, J. W. Jang, K. j. Kong, H. J. Kang, J. Y. Kim, H. Jun, K. Parmar and J. S. Lee, *Angewandte Chemie International Edition*, 2012, **51**, 3147-3151.
49. Y. H. Ng, A. Iwase, A. Kudo and R. Amal, *The Journal of Physical Chemistry Letters*, 2010, **1**, 2607-2612.
50. M. Kato, T. Cardona, A. W. Rutherford and E. Reisner, *Journal of the American Chemical Society*, 2012, **134**, 8332-8335.
51. G. Wang, Y. Ling and Y. Li, *Nanoscale*, 2012, **4**, 6682-6691.
52.Y. Hou, F. Zuo, A. Dagg and P. Feng, *Angewandte Chemie*, 2013, **125**, 1286-1290.
53. Z. Huang, Z. Luo, Y. V. Geletii, J. W. Vickers, Q. Yin, D. Wu, Y. Hou, Y. Ding, J. Song and D. G. Musaev, *Journal of the American Chemical Society*, 2011, **133**, 2068-2071.
54. W. J. Youngblood, S.-H. A. Lee, Y. Kobayashi, E. A. Hernandez-Pagan, P. G. Hoertz, T. A. Moore, A. L. Moore, D. Gust and T. E. Mallouk, *Journal of the American Chemical Society*, 2009, **131**, 926-92755.
55. Thomsen, J. M., Huang, D. L., Crabtree, R. H., & Brudvig, G. W, *Dalton Transactions* 2015, **44**, 12452-12472.
56. S. Roy, M. C. Mourad and M. T. Rijneveld-Ockers, *Langmuir*, 2007, **23**, 399-401.
57. S.-X. Guo, Y. Liu, C.-Y. Lee, A. M. Bond, J. Zhang, Y. V. Geletii and C. L. Hill, *Energy & Environmental Science*, 2013, **6**, 2654-2663.
58.S. Roy, *CrystEngComm*, 2014, **16**, 4667-4676.
59. B. Roy, M. Arya, P. Thomas, J. K. Jürgschat, K. Venkata Rao, A. Banerjee, C. Malla Reddy and S. Roy, *Langmuir*, 2013, **29**, 14733-14742. 60.S. Roy, *Comments on Inorganic Chemistry*, 2011, **32**, 113-126.
61.S. Roy, H. J. Meeldijk, A. V. Petukhov, M. Versluijs and F. Soulimani, *Dalton transactions*, 2008, 2861-2865.
62. P. D. Tran, S. K. Batabyal, S. S. Pramana, J. Barber, L. H. Wong and S. C. J. Loo, *Nanoscale*, 2012, **4**, 3875-3878.
63. H. Li, S. Pang, X. Feng, K. Müllen and C. Bubeck, *Chemical Communications*, 2010, **46**, 6243-6245.
64. A. Iwase, Y. H. Ng, Y. Ishiguro, A. Kudo and R. Amal, *Journal of the American Chemical Society*, 2011, **133**, 11054-11057.
65. S.-S. Li, K.-H. Tu, C.-C. Lin, C.-W. Chen and M. Chhowalla, *ACS nano*, 2010, **4**, 3169-3174.
66. S. Stankovich, D. A. Dikin, R. D. Piner, K. A. Kohlhaas, A. Kleinhammes, Y. Jia, Y. Wu, S. T. Nguyen and R. S. Ruoff, *Carbon*, 2007, **45**, 1558-1565.
67. D. A. Dikin, S. Stankovich, E. J. Zimney, R. D. Piner, G. H. Dommett, G. Evmenenko, S. T. Nguyen and R. S. Ruoff, *Nature*, 2007, **448**, 457-460.
68. D. C. Marcano, D. V. Kosynkin, J. M. Berlin, A. Sinitskii, Z. Sun, A. Slesarev, L. B. Alemany, W. Lu and J. M. Tour, *ACS nano*, 2010, **4**, 4806-4814.
69. W. Hummers and R Offeman *J Am Chem Soc*, 1958, **80**, 1339-1339

New Journal of Chemistry Accepted Manuscript

New Journal of Chemistry Accepted Manuscript



This journal is © The Royal Society of Chemistry 20xx

Please do not adjust margins

## TOC

Enhancement Photochemical water oxidation using as graphene oxide matrix for $[Na_{17}[Mn_6P_3W_{24}O_{94}(H_2O)_2].43H_2O$ @GO] Soft-oxometalate is shown

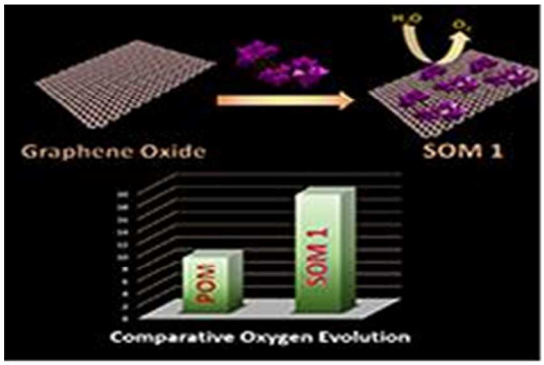


New Journal of Chemistry Accepted Manuscript